JULY 01 2014

Insertion losses of balconies on a building façade and the underlying wave interactions

S. K. Tang; C. Y. Ho; T. Y. Tso

J. Acoust. Soc. Am. 136, 213–225 (2014)
https://doi.org/10.1121/1.4883379

Insertion losses of balconies on a building façade and the underlying wave interactions

S. K. Tang,[a] C. Y. Ho, and T. Y. Tso
Department of Building Services Engineering, The Hong Kong Polytechnic University, Hong Kong, China

(Received 6 June 2013; revised 12 May 2014; accepted 26 May 2014)

This study used scale model experiments to investigate the insertion losses of balconies on a building façade in the presence of ground reflections. The experiments measured both A-weighted broad- and narrowband insertion loss spectra. The underlying wave interactions/interferences and their couplings with and without reflections from the balcony ceilings were also examined in detail, and these findings were related to the dimensions and elevations of the balconies. The findings indicate that the ground and ceiling reflections and their interferences with the direct sound play very important roles in shaping the frequency characteristics of the insertion losses. Strong sound attenuation can be attained with a carefully designed geometry and acoustical properties of the balcony and the balcony ceiling. © *2014 Acoustical Society of America*.
[http://dx.doi.org/10.1121/1.4883379]

PACS number(s): 43.50.Gf, 43.50.Rq [KVH] Pages: 213–225

I. INTRODUCTION

Hong Kong is a densely populated city, with limited flat land for residential purposes that has resulted in many high-rise buildings being built near major ground transportation lines. The current high demand for housing will accelerate the pace of high-rise residential building developments in both the urban and suburban regions.

A balcony without a ceiling provides considerable acoustical protection to the façade behind it.[1] However, evidence from field studies and laboratory investigations (for instance, those of May[2] and Tang[3]) has shown that such protection behind balconies on high-rise building façades is very limited, and noise amplification can result from balcony ceiling reflections. Despite this fact, balconies are welcomed by many people because they can provide an extra living space for various functions that cannot be accommodated by conventional indoor spaces.[4] Therefore, research efforts have been made to investigate the possibility of designing acoustic balconies that can attenuate noise intrusion. Oldham and Mohsan[1] studied such self-protective buildings. El-Dien and Woloszyn[5] investigated the effects that inclined parapets and ceilings have on a balcony's insertion loss. May,[2] Hothersall *et al.*,[6] Lee *et al.*,[7] and Tong *et al.*[8] showed that balconies can provide acoustical protection if they are installed with acoustic treatments. Kropp and Bérillon[9,10] used modal approach to study the low- and mid-frequency noise inside balcony cavities with rigid and non-rigid boundaries. Ishizuka and Fujiwara[11] carried out theoretical analysis and *in situ* measurements regarding the use of concave ceiling panels to improve the acoustical performance of higher floor balconies. El-Dien[12] studied the combined effect of façade and balcony orientation on noise reduction. Naish *et al.*[13] investigated the speech interference levels on balconies affected by road traffic noise. For the improved design of noise-mitigation measures, it is important to understand the acoustical performance of a balcony on a building façade. In the authors' opinion, improving acoustical performance is more challenging when the building façade is not parallel to the major traffic road concerned (that is, the noise source). The main objective of this study is to understand the underlying wave interaction mechanisms.

A 1:3 scale model experiment was carried out to study the insertion loss of balconies (IL). In order to gain a more fundamental understanding of sound propagation into balconies, a single three-story balcony column was used instead of the 3 × 3 balcony array used by Tang[3] and Tang.[14] As explained in previous studies,[3] four symmetrical balcony forms, namely, "Bottom," "Side-Bottom," "Front-Bottom," and "Closed," were included in the experiment. The Bottom balcony consisted of the balcony floor only, and the Closed balcony had both front and side parapets. The Side-Bottom and Front-Bottom balconies contained only the side or front parapets, respectively. It is hoped that the results will provide useful information for the future application of acoustic balconies on high-rise buildings.

II. SCALE MODEL MEASUREMENTS

As in many laboratory studies on the acoustical performances of building elements, such as those of Buratti[15] and Garai and Guidorzi,[16] a single rating in dBA was used in this study to describe the broadband insertion losses of the balconies. Oldham and Mohsan[1] adopted the weightings of Delany *et al.*[17] in their balcony scale model study, but this study used the normalized traffic noise spectrum given in EN1793-3,[18] as road traffic is the main source of noise in Hong Kong.

As the normalized traffic noise spectrum[18] spans from the 100 Hz to the 5000 Hz one-third octave band, a data sampling rate of not less than 38 000 samples per second per channel was required in the 1:3 scale model experiment, and the highest frequency of sound to be measured was

[a]Author to whom correspondence should be addressed. Electronic mail: shiu-keung.tang@polyu.edu.hk

~18 kHz. Figure 1 shows the schematic of the scale model balcony column adopted in this study. The model was made of 20-mm-thick varnished plywood panels, with insignificant sound absorption. The model balconies and the top panels could be removed whenever necessary. A total of 36 equispaced 1/4 in. microphones (Brüel & Kjær type 4956, Denmark) were installed behind each model balcony to capture the sound pressures (and spectra) for the estimation of balcony insertion loss. The span and depth of the balconies are denoted here by l and d, respectively. Owing to the thickness of the plywood panels, the span and depth of the different balcony forms were slightly different (by 20 mm or 40 mm, respectively).

The test chamber was a semi-anechoic chamber with a workable size of 5 m × 4.5 m × 4 m (height). The chamber's walls and ceiling were lined with 2-inch-thick acoustical treatment, and the floor was flat and acoustically hard, to provide ground reflection. The reverberation times between 250 Hz and 5000 Hz were <0.2 s., and those >5000 Hz were <0.1 s. To avoid confusion, the frequencies and the length scales presented hereinafter are scaled back to those associated with the full-size balconies.

The noise source used in this study was a linear loudspeaker array consisting of thirty 6-inch aperture loudspeakers (frequency range: 200 Hz–20 kHz), arranged in six parallel clusters of similar electrical impedance. The perpendicular horizontal distance of the scale model's centerline from the center of the sound source was fixed at 3 m. The centers of the loudspeakers were 104 mm above the floor of the test chamber, so ground reflection has to be taken into account during data analysis. The elevations of the measurement points in the scale model ranged from 5° to 39°. Figure 2 shows the directivities of the sound field at different frequencies, which appear acceptable when compared to those used in previous studies.[3,5,19]

The azimuthal angle, θ, was adjusted by rotating the scale model in an anti-clockwise direction around its central axis. This angle was varied from 0° to 90° in intervals of 15°. As the balconies considered were symmetrical, no measurements were taken in the clockwise θ direction.

It should be noted that the maximum path difference that resulted from the balcony insertion was 10 cm (±0.5 cm) in the scale model. The sound reduction resulting from air absorption within the frequency range of this study was therefore negligible.[20]

III. RESULTS AND DISCUSSIONS

In the foregoing discussions, the broadband IL obtained after applying the normalized traffic noise spectral weighting[16,18] is used in the first place to give an overview of the average ILs of the balconies. These results are relevant to traffic noise insertion loss. Since the insertion losses are frequency dependent, it is therefore also important to understand their spectral characteristics and how the balcony configurations are affecting them. The one-third octave band results will then be presented in order to identify general spectral characteristics and similarities. This will be followed by a detailed narrowband analysis of particular cases, together with a sound propagation model and the possible acoustic model interactions inside the balconies.

A. Broadband ILs

The average broadband ILs behind the balconies were obtained from the logarithmic average sound pressure levels

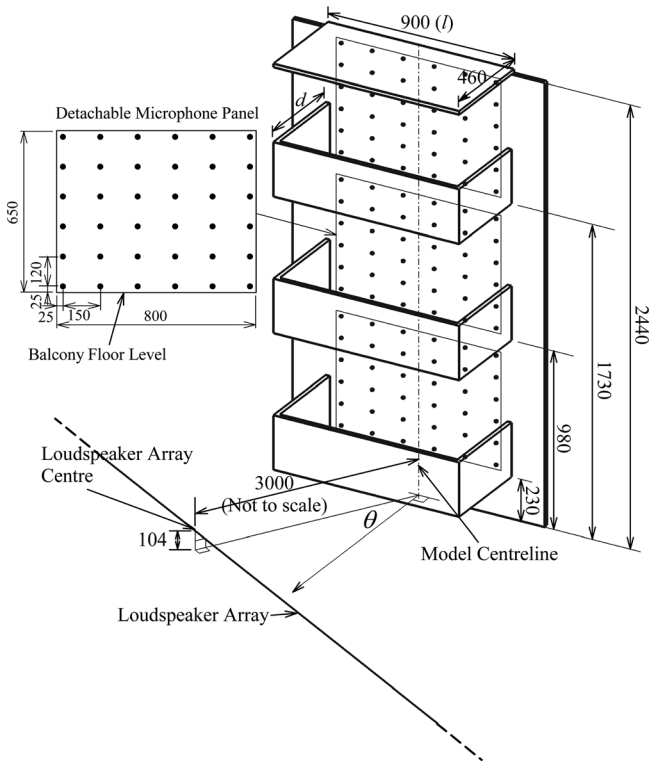

FIG. 1. Schematics of present study and the nomenclature adopted. "•" denotes microphone locations. All dimensions are in mm.

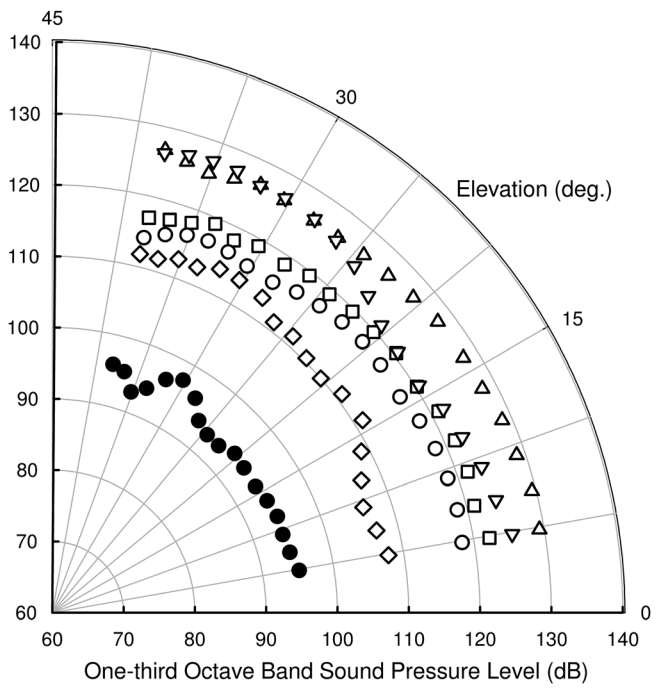

FIG. 2. Sound source directivity (frequency scaled back to real size balcony). (○): 100 Hz; (□): 250 Hz; (△): 500 Hz; (▽): 1000 Hz; (◇): 2500 Hz; (●): 5000 Hz.

measured by the 36 microphones on the model façade, with and without the balconies. A negative IL represents sound amplification.

Figure 3(a) illustrates the ILs behind the top balconies without the balcony ceiling. One can observe that the ILs of the balconies with a front parapet at $\theta = 0°$ are the highest, and they decrease continuously with increasing θ. The front parapet provides the most effective screening at $\theta = 0°$. The Closed balcony provides stronger acoustical protection than the Front-Bottom form, as sound can go directly into the balcony cavity from the two sides of the latter. As θ increases, the screening effect becomes less efficient, especially for the Front-Bottom balcony. At $\theta = 90°$, the front parapet of the Front-Bottom balcony can only screen sound coming from relatively distant noise sources, and thus it can provide only very limited acoustical protection.

For the balconies without a front parapet, a slightly increasing trend of IL with θ can be observed, but the trend associated with the Bottom balcony is insignificant. At $\theta = 0°$, the side parapets of the Side-Bottom balcony act as acoustic fins, but sound can easily enter the balcony cavity due to the absence of a front parapet. The mixture of sound reflections within the balcony cavity and the possibility of standing wave setup together make the performance of the Side-Bottom balcony not much better than that of the Bottom balcony at this azimuthal angle. One of the side parapets acts as a direct sound barrier when θ increases, and its maximum protection performance takes place at $\theta = 90°$.

Figure 3(a) also shows that the performances of the Front-Bottom and Side-Bottom balconies cross each other at θ of between 45° and 60°. This crossover orientation may be related to the aspect ratio of the balcony floor, but that question is left for further investigation. The performance of the Front-Bottom balcony is also slightly worse than that of the Bottom balcony when θ is large. Again, the sound reflection and standing waves between the façade and the front parapet of the Front-Bottom balcony form play a role in this.

To the best of the authors' knowledge, few previous studies have gathered data from *in situ* observations of balcony insertion loss, as measured by observing the differences between sound levels with and without the balcony. However, there have been a number of scale-model studies, as mentioned above. It should be noted that the average sound propagation path difference that resulted from the insertion loss of the top Closed balcony is ~0.2 m (effective path difference is ~0.15 m, as calculated according to Oldham and Mohsen[1]). The insertion loss of the Closed balcony, which Oldham and Mohsen[1] obtained by using a scale model of similar size at $\theta = 0°$ and with a similar effective path difference, is ~5.5 dBA (see Fig. 17 of Oldham and Mohsen[1]). That is in good agreement with the result of this study.

As shown in Fig. 3(b), the presence of ceiling reflections largely reduces the insertion losses of the top balconies. The insertion losses of the four balcony types are very similar, especially at $\theta \leq 45°$. Such losses are insignificant and

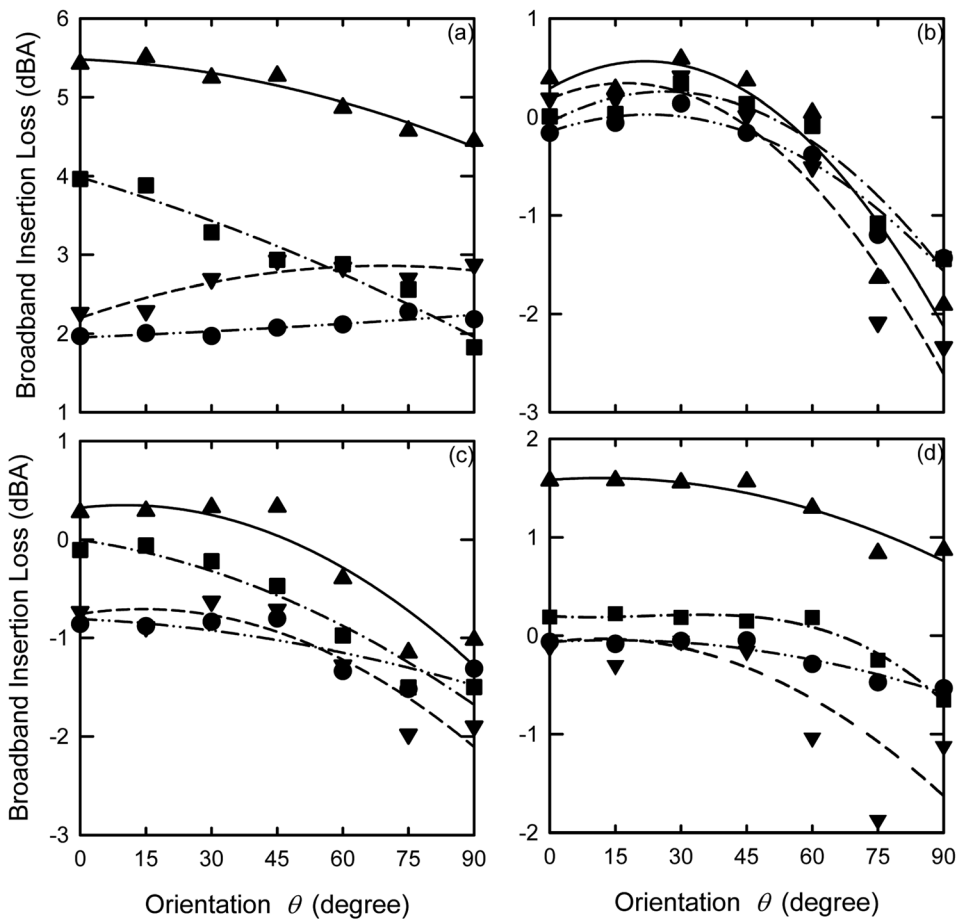

FIG. 3. Variations of single rating insertion losses with azimuthal angle. (a) Top balconies without ceiling; (b) top balconies with ceiling; (c) middle balconies with ceiling; (d) bottom balconies with ceiling. (●): Bottom; (■): Front-Bottom; (▲): Closed; (▼): Side-Bottom. Regression lines: —, Closed; –·–, Front-Bottom; –··–, Bottom; —, Side-Bottom.

basically unchanged within this azimuthal angle range. The ceiling reflects sound into the cavity, and such reflection diminishes the screening effects of the balcony floors and the parapets. Sound amplification is observed at $\theta \geq 60°$ for three of the four balcony forms. The balconies with side parapets give the largest amplification as θ increases toward 90°. At large θ and in the presence of ceiling reflection, the side parapets tend to trap more sound energy inside the balcony cavity, resulting in higher sound intensity and even amplification there. This amplification will be further discussed later.

Figure 3(c) illustrates the insertion losses of the middle-level balconies. Sound amplification is observed for all balcony forms except for the Closed form, but the insertion loss of the Closed form is also insignificant. Sound amplifications behind the middle balconies are all stronger than those behind the top balconies, but the difference becomes smaller as θ increases toward 90°. The observed increase in amplification associated with the balconies without front and/or side parapets is due to the weaker diffraction losses at the middle level than those measured for the top-level balconies and the stronger reflection from the balcony ceilings.

Figure 3(d) presents the insertion losses behind the bottom-level balconies. The corresponding ILs are basically constant for $\theta \leq 45°$. Again, the side parapets appear to have a deterministic effect on the sound insulation. The ILs decrease with increasing θ for $\theta \geq 60°$, but a small rebound can be observed for the Bottom balcony at $\theta = 90°$. In fact, similar but much smaller rebounds can also be observed in the cases of the middle balconies. However, the rebound magnitudes are insignificant in practice.

One can notice from Figs. 3(c) and 3(d) that the ILs of the lowest balconies are higher than those of the middle balconies. This pattern has been confirmed by repeated experiments. The phenomenon probably results from the reduction of the ceiling reflection within the bottom-level balconies, which are at lower elevations. As can be observed in Fig. 3(d), the Bottom balcony is the least sensitive to azimuthal angle change among the four balcony forms tested in this study.

The sound field patterns behind the balconies are not uniform, and so the patterns of insertion losses also varied. Figure 4 presents the broadband IL contour maps behind the top balconies at different θ (as viewed from the front of the model) in the presence of the reflective ceilings. One should note that the heights of these maps span from 225 mm to 2025 mm above the balcony floor (Fig. 1). These are the regions in which the microphones were located.

It is obvious that the Bottom balcony form will give the least acoustical protection and the IL will increase with height above balcony floor in the absence of ceiling reflection, in general. Thus, the corresponding results are not presented. Figure 4 shows that ceiling reflection results in sound amplification over the upper half of the façade behind the top balconies when θ is small regardless of the balcony forms. The amplification zone extends downward and is slightly biased toward the right-hand side as θ increases, because of the larger reflected sound power into the balcony

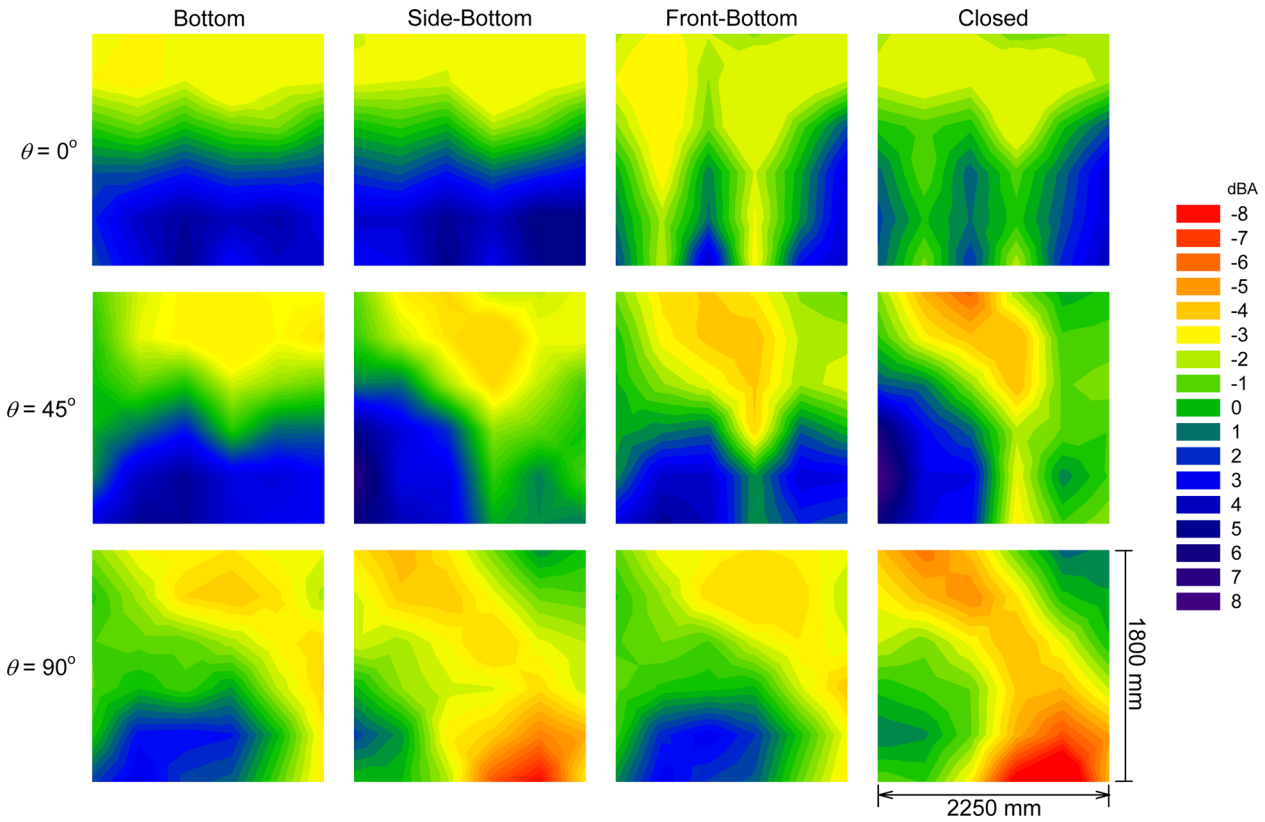

FIG. 4. (Color online) Single rating insertion loss maps of the top balconies in the presence of ceiling reflection.

cavity that resulted from the 2.7-m-long balcony ceiling. At $\theta = 90°$, acoustical protection can only be found in the region near to the balcony's leading edge and its floor, where the effects of the reflected sound power are relatively less significant. This applies to all four balcony forms.

One can also observe from Fig. 4 that at small θ, the broadband IL maps behind balconies without and with a front parapet show two distinctive characteristics. In the presence of a front parapet, some standing-wave-like patterns are found. These patterns are more distinctive in the region below the top edge of the front parapet. At large θ, however, the side parapets basically determine the IL distribution pattern. For the balconies with side parapets, a strong sound amplification region is found at the lower right-hand corner of the balcony void because of the sound reflections at the ceiling and the side parapet. Such amplification zone is missing in balconies with only a front parapet as the sound reflected by the ceiling and/or diffracted by the left-hand-side parapet leaves the balconies on the right-hand side. The Closed balconies have the advantages of both front and side parapets. As the parapets are sound barriers by themselves, the lower half of the balcony cavity is well shielded against noise. However, the reverberation and acoustic modes within the balcony cavity can reduce the average IL. This effect will be further discussed later in Sec. III C.

The IL distribution patterns inside the middle- and bottom-level balconies basically follow those presented in Fig. 4, but with wider amplification zones and smaller IL spatial variations, in general. The corresponding data are, thus, not presented here.

B. One-third octave band ILs

Figure 5 illustrates the average one-third octave band insertion losses on the façades behind the balconies at $\theta = 0°$, 45°, and 90°. At $\theta = 0°$, in the absence of ceiling reflection [Fig. 5(a)], all of the microphones behind the top balconies are within the shadow zone of the front parapet in the cases of the Closed and Front-Bottom balconies. One can observe that the performances of the Side-Bottom and Bottom balconies are very comparable, and similar phenomenon is found behind the Front-Bottom and Closed balconies, though the latter give slightly higher ILs. The front parapet thus controls the general balcony screening characteristics at this top elevation level in the absence of ceiling reflection, especially at frequencies >500 Hz, because of the increasing Fresnel number.[21] It appears that, on average, the presence of the side parapets give an ~1.5 dB increase in the IL in this frequency range.

A relatively strong IL peak is found within the 100 Hz one-third octave band for all balcony forms included in this study. The corresponding IL contours show low pressure regions in the central regions of the façades behind these balconies, and the locations of lowest sound pressure levels

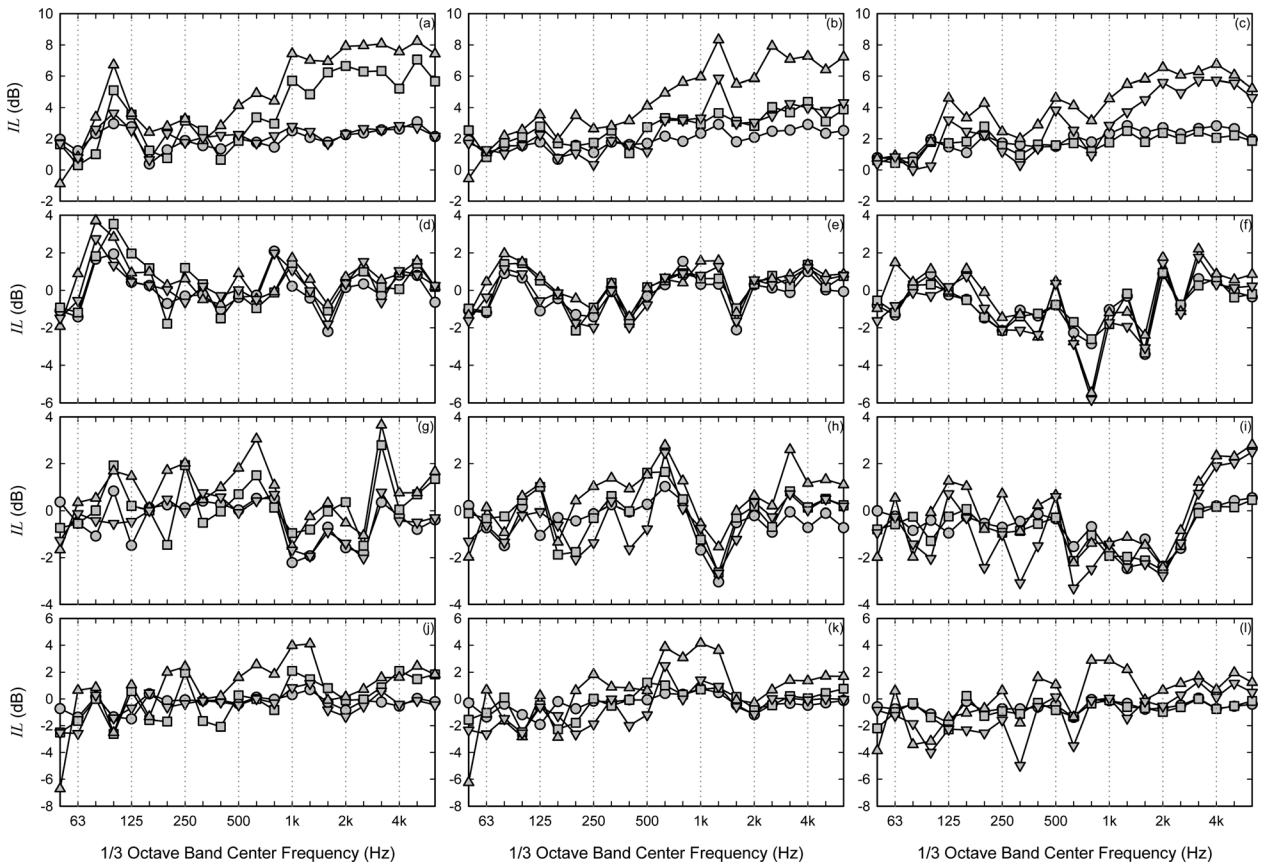

FIG. 5. One-third octave band insertion loss spectra. (a),(b),(c) Top balconies without ceiling at $\theta = 0°$, 45°, and 90°, respectively; (d),(e),(f) top balconies with ceiling at $\theta = 0°$, 45°, and 90°, respectively; (g),(h),(i) middle balconies with ceiling at $\theta = 0°$, 45°, and 90°, respectively; (j),(k),(l) bottom balconies with ceiling at $\theta = 0°$, 45°, and 90°, respectively. (•): Bottom; (■): Front-Bottom; (▲): Closed; (▼): Side-Bottom.

are usually near the centers of these façades (not shown here). As this IL peak appears for all of the balcony forms, it is probably due to the effect of the balcony floor. This IL peak will be further discussed later.

As shown in Figs. 5(b) and 5(c), the 100 Hz IL peak disappears at $\theta \geq 45°$. The asymmetrical edge diffraction appears to have allowed more sound into the balcony cavity. At $\theta = 45°$, the performances of the Front-Bottom and the Side-Bottom balconies are very similar over the whole traffic noise frequency range. A strong IL peak appears at the 1250 Hz one-third octave band behind the balconies with side parapets. Such an IL peak, though with a smaller magnitude, can also be observed in Fig. 5(a), even for the case of the Front-Bottom balcony where the front parapet and the façade together form a sound propagation channel. At $\theta = 90°$ [Fig. 5(c)], the front parapet at this top elevation level is not useful, and thus the Front-Bottom balcony performs no better than the Bottom balcony over the measured frequency range. The one-third octave band ILs of Front-Bottom and Bottom balconies are nearly unchanged at about 2 dB for frequencies >100 Hz. For the Side-Bottom and Closed balcony forms, clear and relatively regular IL peaks and dips can be observed. Again, it is expected that the acoustic modes, wave interferences, and resonances are important, which will be further discussed later.

As shown in Figs. 5(d)–5(f), the presence of ceiling reflection in the top balconies substantially reduces the acoustical benefit resulting from the parapets and balcony floors. The 100 Hz IL peak seen in Fig. 5(a) can basically be found in Fig. 5(d), but the magnitudes of such peaks associated with the balconies having a front parapet are similar to those of the others. The reflected energy from the ceiling results in lower insertion loss across the measured frequency range, and even sound amplification at many frequencies above the 125 Hz one-third octave band. Relatively significant insertion loss can only be found at around the 80–125 Hz frequency bands. The four balcony forms give nearly identical performances at $\theta = 45°$ [Fig. 5(e)]. A very prominent sound amplification is observed within the 800 Hz band at $\theta = 90°$ behind balconies with side parapets [Fig. 5(f)], which is probably due to the type of multiple reflections that take place between the balcony ceiling, the leeward side parapet, and the balcony floors shown in the lower right-hand corner subfigure of Fig. 4. In fact, a small IL dip can also be found around the 315 Hz and 400 Hz bands. IL dips can be found at the 1600 Hz and the 2500 Hz bands, and IL peaks can be observed at the 1250 Hz and 2000 Hz bands for all four balcony forms tested. The long ceiling span in the direction of sound propagation ($\theta = 90°$) reflects sound energy into the balcony cavities, and it appears that such reflection is coupled with some resonances and/or interferences associated with a ~400 Hz sound and its harmonics. This coupling of reflections and resonances will be further discussed later.

The middle balcony ceiling reflects more sound energy into the balcony cavity than those of the top or the bottom-level balconies. As shown in Figs. 5(g)–5(i), the ILs of the balconies become highly frequency dependent, probably because of the stronger excitations of cavity modes, wave interferences, and resonances. The results for the balconies with vertical parallel reflecting surfaces are relatively choppy. Again, the IL dips and peaks are at frequencies with harmonic relationships, which indicate that resonances and interferences are important in shaping the insertion losses of these balconies.

Figures 5(j)–5(l) illustrate the one-third octave band insertion loss spectra behind the bottom-level balconies at different θ. At this low elevation level, the ceiling reflection is considerably weaker than those occurring in the middle and top balconies. The fluctuations of IL are also less serious, but those associated with balconies having vertical parallel surfaces facing in the direction of major sound propagation remain relatively strong, probably because of mode excitations and the possible resonances and interferences.

C. Narrow band IL spectra and wave interactions

In this section, a narrow bandwidth spectral analysis is carried out to investigate the resonances, wave interferences, and various modes that affect balcony insertion losses. For the sake of easy reference, Fig. 6 summarizes the wave interaction mechanisms that should be taking place in the balconies and affecting their insertion losses. These mechanisms are hereinafter referred to as M0–M7. Table I lists the eigenfrequencies of the horizontal cross-sections of the Closed and Front-Bottom balconies. Acoustic modes are not expected to be influential inside the Side-Bottom and

Schematics	Code	Critical Frequencies, f	Remark
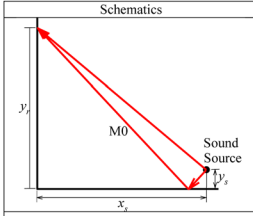	M0	Interference path difference δ $= \sqrt{x_s^2 + (y_r + y_s)^2} - \sqrt{x_s^2 + (y_r - y_s)^2}$, and $f = pc/(2\delta)$, where p is an integer.	Take place on façade without balcony. Constructive interference when p is even; destructive otherwise.
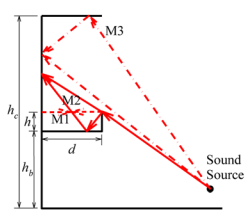	M1	Resonance frequency $f = pc/(2d)$	Due to wave diffracted at the edge of the front parapet and floor.
	M2	Interference path difference δ $= \sqrt{d^2 + (y_r - h_b - h)^2} - \sqrt{d^2 + (y_r - h_b + h)^2}$ and $f = pc/(2\delta)$.	Due to diffraction at balcony parapet edge and balcony floor reflection. Constructive interference when p is even; destructive otherwise.
	M3	Interference path difference δ $= \sqrt{x_s^2 + (2h_c - y_r - y_s)^2} - \sqrt{x_s^2 + (y_r - y_s)^2}$, and $f = pc/(2\delta)$.	Due to ceiling reflection and direct sound. Constructive interference when p is even; destructive otherwise
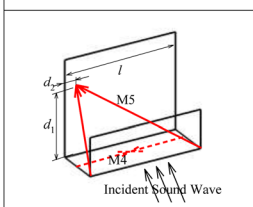	M4	Resonance frequency $f = pc/(2l)$	Due to diffracted waves at the floor edges. p is an odd integer for small θ.
	M5	Interference path difference δ $= \sqrt{d_1^2 + (l - d_2)^2 + d^2} - \sqrt{d_1^2 + d_2^2 + d^2}$ and $f = pc/(2\delta)$.	Due to diffracted sound from the edge of the floor and parapets (side and front). Constructive interference when p is even; destructive otherwise.
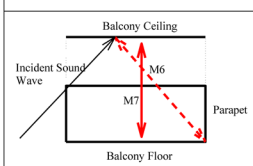	M6	Resonance frequency $f = \frac{pc}{2\sqrt{A^2 + (h_c - h_b)^2}}$, $A = \frac{(x_s + l/2)(h_c - h_b)}{2h_c - h_b - y_s}$.	Take place at large θ in balconies with side parapets.
	M7	Resonance frequency $f = pc/[2(h_c - h_b)]$	

FIG. 6. (Color online) Schematics of wave interaction mechanisms.

TABLE I. Eigenfrequencies of Front-Bottom and Closed balcony cavity horizontal cross-sections below 1000Hz[a] (m: spanwise order; n: depthwise order. Speed of sound, $c = 343$ m/s. $f_{m,n} = 0.5c\sqrt{(m/l)^2 + (n/d)^2}$).

m	n	0	1	2	3	4	5	6
0		0	136.1 (136.1)	272.2 (272.2)	408.3 (408.3)	544.4 (544.4)	680.6 (680.6)	816.7 (816.7)
1		63.5 (66.5)	150.2 (151.5)	279.5 (280.2)	413.2 (413.7)	548.1 (548.5)	683.5 (683.8)	819.1 (819.4)
2		127.0 (133.0)	186.2 (190.3)	300.4 (303.0)	427.6 (429.4)	559.1 (560.4)	692.3 (693.4)	826.5 (827.4)
3		190.6 (199.4)	234.2 (241.4)	332.3 (337.5)	450.6 (454.4)	576.8 (579.8)	706.7 (709.2)	838.6 (840.7)
4		254.1 (265.9)	288.2 (298.7)	372.4 (380.5)	480.9 (487.3)	600.8 (605.9)	726.4 (730.7)	855.3 (858.9)
5		317.6 (332.4)	345.5 (359.2)	418.3 (429.6)	517.3 (526.5)	630.3 (637.9)	751.0 (757.4)	876.2 (881.7)
6		381.1 (398.8)	404.7 (421.4)	468.3 (482.9)	558.6 (570.8)	664.6 (674.9)	780.0 (788.8)	901.2 (908.9)
7		444.6 (465.3)	465.0 (484.8)	521.3 (539.1)	603.7 (619.1)	702.9 (716.2)	812.9 (824.4)	929.9 (939.9)
8		508.1 (531.8)	526.1 (548.9)	576.5 (597.4)	651.9 (670.5)	744.7 (761.1)	849.3 (863.7)	961.9 (974.5)
9		571.7 (598.3)	587.6 (613.5)	633.2 (657.3)	702.5 (724.3)	789.4 (808.9)	888.8 (906.1)	996.9 (1012.4)
10		635.2 (664.7)	649.6 (678.5)	691.1 (718.3)	755.1 (780.1)	836.6 (859.2)	930.9 (951.3)	
11		698.7 (731.2)	711.8 (743.8)	749.9 (780.2)	809.3 (837.5)	885.8 (911.6)	975.4 (998.9)	
12		762.2 (797.7)	774.3 (809.2)	809.4 (842.8)	864.7 (896.1)	936.7 (965.8)		
13		825.7 (864.1)	836.9 (874.8)	869.5 (906.0)	921.2 (955.8)	989.1 (1021.4)		
14		889.3 (930.6)	899.6 (940.5)	930.0 (969.6)	978.5 (1016.3)			
15		952.8 (997.1)	962.5 (1006.3)	990.9 (1033.6)				

[a]Data in parentheses: Closed balcony form.

Bottom balconies, and thus their eigenfrequencies are not presented.

Figure 7 presents the insertion loss spectra of some important top balcony cases in the absence of ceiling reflection. The frequency resolution is 2.67 Hz. In addition to the averaged data from all 36 microphones, the figure also presents averaged data obtained from the upper and lower halves of the model façade, to help show the contributions of the cavity modes to the overall acoustical protection of the balconies.

The situation of the Bottom balcony form is the simplest, as no significant cavity mode resonance can take place within this balcony. The balcony floor acts like a rectangular sound barrier. As shown in Fig. 7(a), the insertion losses at $\theta = 0°$ are relatively uniform over the façade surface at frequencies below 500 Hz. Only significant insertion losses can be found within the lower half of the protected façade at frequencies > 500 Hz. In the high frequency range, apart from a very spurious IL frequency variation, the IL increases with frequencies, in general, because of the sound barrier effect.[22]

Diffraction takes place as sound waves hit the balcony floor edges.[22,23] Along the front edge, some sound is diffracted toward the model façade, and is subsequently reflected back (M1). Weak resonances could then occur at frequencies near to an integer multiple of $c/(2d)$, where c is the ambient speed of sound, leading to a lower IL. As in-phase diffraction generally takes place at the side edges, diffraction grating will be formed on the façade. Resonance along the balcony span (M4) could take place at frequencies close to an odd integer multiple of $c/(2l)$. In addition, there is interference between sound radiated directly from the source and that reflected from the hard ground of the test chamber, making the insertion loss highly frequency dependent, as illustrated by Lam and Roberts.[23] This is mechanism M0. However, such interference at the diffracting front balcony floor edge does not significantly affect the overall IL at $\theta = 0°$, as similar interference is also taking place on the façade in the absence of the balcony, though at slightly different frequencies. Therefore, such interference will not be further discussed except in special situations.

In Fig. 7(a), the frequencies related to the integer multiple of $c/(2l)$ are indicated with the symbol "↓." The upper and lower ↓ rows denote frequencies equal to the odd and even integer multiples of $c/(2l)$, respectively. Those frequencies related to the integer multiple of $c/(2d)$ are marked with "↑." Although the noise source used in the experiment was not a perfect line source, the chance of having a local IL dip at the frequency near to the symmetric spanwise resonance frequencies is high, especially at lower frequencies. The resonance, although not expected to be strong here, tends to strengthen the sound fields, resulting in a relatively lower IL. In the low frequency range, the asymmetric spanwise resonance frequencies are close to those of the depthwise resonance. The asymmetric acoustic resonances along the balcony span do not match with the boundary condition at the two sides of the balcony. This effect tends to counteract with the resonance along the depthwise direction of the balcony (M1). At higher frequencies, there are cases in which the symmetrical spanwise resonance frequencies are midway between two adjacent depthwise resonance frequencies (when $2d$ equals approximately an odd multiple of half the wavelength), or a depthwise resonance frequency is located between a symmetric and an asymmetric spanwise resonance frequency pair. The magnitude of the IL then depends on the relative strength of these two effects. There are many cases in which the symmetric spanwise resonance frequencies are near to the depthwise resonance frequencies. Significant IL dips are usually found in those cases (e.g., at ~1830 Hz, ~2600 Hz, ~3500 Hz).

An IL peak and IL dip are observed around 112 Hz and 93 Hz, respectively, and it appears that the corresponding

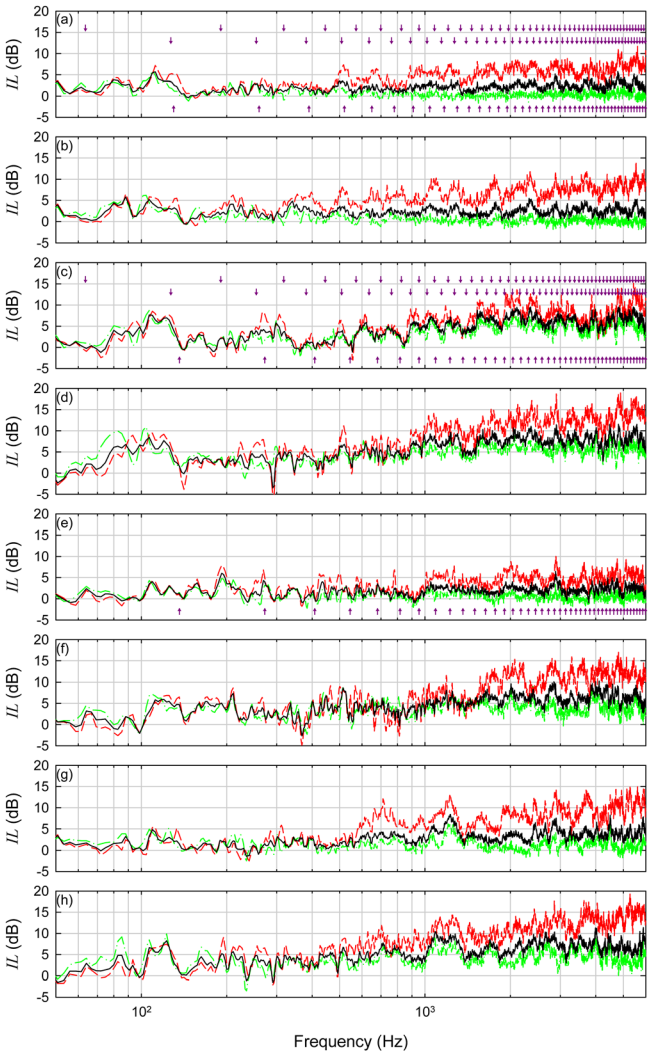

FIG. 7. (Color online) Insertion loss spectra of top balconies without ceiling. (a) Bottom balcony at $\theta = 0°$; (b) Side-Bottom balcony at $\theta = 0°$; (c) Front-Bottom balcony at $\theta = 0°$; (d) Closed balcony at $\theta = 0°$; (e) Front-Bottom balcony at $\theta = 90°$; (f) Closed balcony at $\theta = 90°$; (g) Side-Bottom balcony at $\theta = 45°$; (h) Closed balcony at $\theta = 45°$. ————: Average IL; — — — —: lower façade average IL; –·–: upper façade average IL. (↑): depthwise resonance frequencies; (↓): spanwise resonance frequencies.

insertion losses are relatively uniform over the balcony façade. From a rough two-dimensional estimation, the horizontal distance between the balcony floor corner and the middle of the façade is 1.847 m. At this elevation level, most of the sound goes into the balcony region through diffractions at the parapet and/or floor edges (M5). A resonance can then take place at ~93 Hz, resulting in relatively high sound pressure in the middle region of the balcony façade, thus causing the observed IL dip. The reason for the 112 Hz IL peak is unclear. This frequency is not associated with any of the abovementioned modes or interferences. Destructive interference between the diffracted sounds from the side edges and front edge of the balcony is also not possible at this frequency because of the small difference in the lengths of the corresponding propagation paths. However, the ~5 dB insertion loss at this frequency appears to agree very well with that of the infinitely long sound barrier at a similar Fresnel number (average ~ 0).[21] For a finite length barrier, vertical edge diffraction reduces the insertion loss at low frequencies.[23] It is likely that the diffractions from the two side edges of the balcony counteract with each other, diminishing the overall contribution of side edge diffraction in the overall sound field inside the balcony region. As discussed previously, in the one-third octave band analysis, the insertion loss at the 100 Hz band peaks around the middle-height level of the balcony façade. The distances from a balcony floor corner to a location at mid-balcony height on the façade edge opposite to that corner and to a similar location on the façade edge near to that corner are 3.21 m and 1.74 m, respectively. Destructive interference between these diffracted sounds will then occur at around 116 Hz (M5). This frequency increases with height within the balcony, but decreases as the diffraction point on the side edge is closer to the façade. The frequency range is approximately from 101 Hz to 140 Hz.

Figure 7(b) illustrates the frequency variations of IL behind the top Side-Bottom balcony at $\theta = 0°$ in the absence of ceiling reflection. The characteristics of these IL variations are basically similar to those of the corresponding case of the Bottom balcony [Fig. 7(a)]. In fact, the abovementioned resonant behaviors are more obvious in this case, indicating that physical wave interaction mechanisms similar to those seen in the top Bottom balcony case also take place inside the Side-Bottom balcony. The side parapets provide some noise screening effects in the lateral directions, but also allow for multiple reflections within the balcony cavity. The latter may give rise to standing waves, but they should be weak because the balcony cavity is relatively open to the surroundings. The very similar Figs. 7(a) and 7(b) suggest that the side parapets do not have a very significant effect on the spectral characteristics of IL.

The Front-Bottom balcony at $\theta = 0°$, in the absence of ceiling reflection, produces higher IL on the upper half of the model façade at frequencies > 500 Hz than does the Side-Bottom or Bottom balconies, because of the screening effect of the front parapet [Fig. 7(c)]. However, the more intense sound reflections and reverberations within this more confined balcony cavity result in an overall IL in the lower half of the model façade not better than that in the Side-Bottom and Bottom balconies, despite the stronger screening effect of the front parapet. The reflections within the space between the front parapet and the façade also create severe interference, which further complicates the sound field distribution on the façade. However, one can still observe that there is a higher chance of having a local IL dip at or close to a depthwise resonance frequency (M1), especially in the low frequency range. IL peaks and dips are also very often found at the egienfrequencies of asymmetric and symmetric spanwise cavity modes, respectively. It should be noted that some of the asymmetric mode frequencies are very close to those of the symmetric modes at high frequencies (Table I), which make the contributions of individual modes indistinguishable in the presence of serious modal overlapping. The corresponding data are thus not further discussed. However, it appears that the depthwise resonance is relatively more important in creating the IL dips.

One can observe that there are two relatively prominent IL peaks at ~272 Hz and 300 Hz. The latter peak is near an asymmetric lateral mode of the balcony cavity, which should have been weak (see Table I; $m = n = 2$). The former peak is, in fact, close to c/d, and thus should result in a high sound-pressure region on the façade and an IL dip. However, it should be noted that there are multiple reflections within the balcony cavity between the façade, the parapet, and the balcony floor. For a source at the front parapet edge (cf. Huygens' principle[24]), destructive interferences between diffracted waves and those reflected by the balcony floor within the frequency range from 150 Hz to 350 Hz can be found on the balcony façade (M2). Such interference takes place at a height of 0.6 m above the balcony floor for a 272 Hz sound, and thus the average sound pressure level at the lower half of the façade is low, and a local IL peak resulted below the height of the parapet. The kind of side-edge diffraction interferences shown in Fig. 7(a) for the Bottom balcony also apply to this Front-Bottom balcony case, and thus the IL peaks at around 110 Hz. However, the IL dip at ~93 Hz is only found in the upper half of the façade in Fig. 7(c), probably because of the screening effect of the front parapet.

The co-existence of side and front parapets on a balcony further complicates the sound field inside the balcony cavity, especially at the lower half of the façade where both the IL features associated with these parapets can be found [Fig. 7(d)]. These parapets cause very spurious IL frequency variations. The average IL is very broadband and relatively constant at ~5–6 dB at frequencies > 500 Hz. At lower frequencies, the IL is also generally the highest among all of the balcony forms tested. In general, it can be observed that some IL features associated with the side and front parapets counteract each other, giving rise to relatively uniform IL, except at some frequencies in which strong IL dips can be found due to mode excitations (cf. Table I). The very strong and sharp IL dip at ~292 Hz seems to be a result of the excitation of the $(m,n) = (4,1)$ symmetrical spanwise mode of the Closed balcony. Another relatively sharp dip is observed at 345 Hz, which is near the $(m,n) = (5,1)$ symmetric spanwise mode of the Front-Bottom balcony cavity. The latter mode is not expected within a balcony cavity bounded by rigid walls, but it is likely to function at a height level near that of the parapet edges, resulting in an IL dip around the middle part of the façade (not shown here). At frequencies < 200 Hz, the IL performance is similar to that of the Front-Bottom balcony, and thus it is not further discussed.

At $\theta = 90°$, in the absence of ceiling reflection, balcony performance is critically affected by the side parapets, as shown in Fig. 5(c). Thus, only the corresponding IL spectra of the Front-Bottom and Closed balconies will be presented [in Figs. 7(e) and 7(f), respectively]. At this orientation of grazing incidence, the IL of the Front-Bottom balcony is weak across the measured frequency range. It should be noted that both symmetric and asymmetric modes, be they of the spanwise or the depthwise types, can be excited in this case because of the asymmetric balcony setup relative to the sound source. However, the symmetric depthwise modes are still more effectively excited.

One can observe from Fig. 7(e) that an IL peak is generally not likely to appear at the frequency of a purely depthwise direction resonance, though there are limited peaks at ~270 Hz and ~680 Hz. At low frequency, the IL peaks appear at ~63 Hz (minor), 127 Hz, 150 Hz, 193 Hz, 270 Hz, and 300 Hz, and the dips appear at ~175 Hz, 238 Hz, 317 Hz and 380 Hz. There are small upward "kicks" at 136 Hz and 279 Hz in the average frequency variation of the average lower half façade IL. It is interesting to note that all of these frequencies are very close to the lower order eigenmode frequencies of the balcony cavity (Table I). The dip frequencies are more related to the higher order spanwise modes ($m \geq 3$), and those of the peaks mainly to those with $m < 3$. Similar phenomena are not clearly observed at $\theta = 0°$ [Fig. 7(c)]. The likely cause is the direct sound propagation into the balcony cavity at $\theta = 90°$ such that the modal characteristics of the balcony cavity, especially the depthwise symmetrical characteristics, become more influential in the sound field inside this region. These peaks and dips also appear in the Bottom balcony case, but are of slightly lower magnitudes. The balcony floor thus plays an important role in affecting the IL, and the front parapet strengthens the effect. Further investigation of these effects is required. The peak at ~270 Hz is probably due to the destructive interference from waves diffracted at the front parapet edge [Fig. 7(c); M2].

At higher frequencies, modal overlapping is very serious, and thus the corresponding results are not further discussed because of the high degree of uncertainty. The co-excitations of many spanwise modes with odd and even values of m can also reduce the overall sound level on the façade. One example can be found at ~575 Hz, at which modes of $m = 8$ and 9 with even n are excited (Table I). Another example is the relative broadband dip at ~930 Hz, at which many modes of even m are excited. The small peak at 680 Hz mentioned above coincides with two asymmetric depthwise modes of $n = 5$ ($m = 0$ and 1). It should also be noted that the sound transmission will be further affected by the phase of the sound reaching the two balcony floor side edges. The path difference here is 2.34 m. The dip at 234 Hz could be due to the path difference effect, as the sounds reaching the two side edges are roughly out-of-phase at 220 Hz, and this tends to favor the propagation of a spanwise mode with odd m (M4). The opposite may have occurred at 175 Hz, with the nearest mode having $m = 2$, $n = 1$, and an in-phase condition between the sounds reaching the side edges is roughly achieved at 175 Hz. The exact in-phase condition is at 147 Hz, which is close to the frequency of the $(m,n) = (1,1)$ mode. The mismatch in the wave pattern tends to reduce the sound transmission along the balcony cavity, and thus the IL peaks at ~150 Hz. Further investigation of this pattern is required.

As Fig. 7(f) shows, the IL frequency variation of the Closed balcony at grazing incidence is much more spurious than that of the Front-Bottom balcony, because of the more serious cavity mode effects, either inside the cavity or around the height of the parapet. With the side parapets in place, the asymmetric depthwise modes are just as important as their symmetric counterparts. There are complicated wave interactions, but the lower order eigenmode frequencies of

the cavity, in this case, match reasonably well with those in which the IL dips below 900 Hz before modal overlapping becomes too serious for drawing reasonable conclusions.

Although the large dip at ~370 Hz is probably due to the excitation of a cavity mode (Table I), the peak at 210 Hz cannot be associated with any acoustic mode. Such a peak is not observed in the Side-Bottom balcony case, and thus its presence is primarily due to the front parapet. As shown previously in the Front-Bottom balcony case, a destructive interference associated with the diffraction at the front parapet edge affects the sound field (M2). Destructive interference at 210 Hz takes place at a height of ~0.8 m from the balcony floor (parapet height 0.84 m). It should be noted that although such kinds of interference can take place at slightly higher frequencies, the effects will not be prominent as the location of destructive interference will be deeper inside the balcony cavity, where the multiple reflections and reverberation tend to smooth out nodal points.

The average IL spectra at $\theta = 45°$ in the absence of ceiling reflection behind the Side Bottom and Closed balconies are shown in Figs. 7(g) and 7(h), respectively. The kinds of wave interaction discussed above is not straightforward in these cases. Taking the Closed balcony as an example, a drop in the IL can be observed at ~100 Hz, but some IL peaks are unchanged, even in magnitude, when θ increases from 0° to 45°. The variation of IL spectra with azimuthal angle is complicated, and detailed discussions of the corresponding results have to be given in a separate report because of page limitations.

The ceiling reflection lowers the IL of the balconies substantially. Some examples of the corresponding IL spectra are presented in Fig. 8. At $\theta = 0°$, the performances of the top Front-Bottom and Bottom balconies are similar to those of the top Closed and Side-Bottom balconies [Fig. 7(d)], and thus only the ILs of the Closed and Side-Bottom balconies are presented [in Figs. 8(a) and 8(b), respectively]. For the Closed balcony, the ceiling reflection nearly erases the acoustical protection provided by the parapets and balcony floor at frequencies >100 Hz, even though the IL can be maintained at ~110 Hz within the lower half of the façade. The dips in IL at frequencies <500 Hz can also be found in the case without ceiling reflection [Fig. 7(d)], which suggests that similar wave mechanisms take place in the presence of ceiling reflection, and thus they are not further discussed.

Modal overlapping tends to make the contributions from different modes at higher frequencies indistinguishable. The average IL depends on how these modes interact with each other, and thus the insertion loss is not predictable except in limited specific cases. One example is at 2349 Hz, where a relatively strong IL peak is found, and the corresponding average ILs on the upper and lower half of the façade are very similar. This frequency is actually close to the eigenfrequencies of many asymmetric spanwise cavity modes, which should not be forced out effectively, which explains the relatively large IL peak.

The frequency variations of ILs behind the top Side-Bottom balcony at $\theta = 0°$ are shown in Fig. 8(b). Without the front parapet, the sound field on the upper half of the façade is generally broadband amplified under the presence

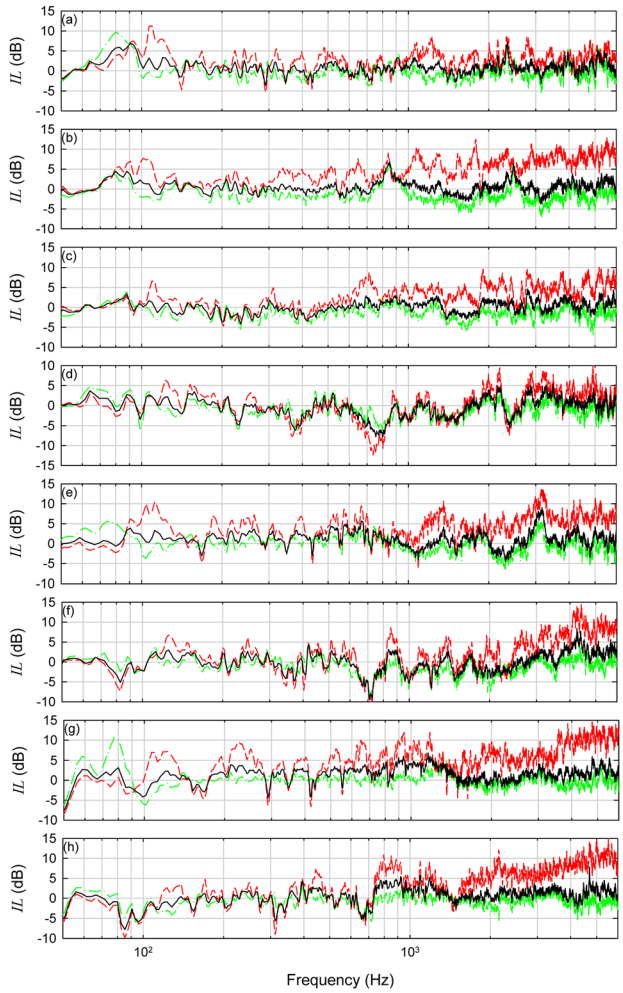

FIG. 8. (Color online) Insertion loss spectra of balconies with ceiling. (a) Top Closed balcony at $\theta = 0°$; (b) top Side-Bottom balcony at $\theta = 0°$; (c) top Side-Bottom balcony at $\theta = 45°$; (d) top Closed balcony at $\theta = 90°$; (e) middle Closed balcony at $\theta = 0°$; (f) middle Closed balcony at $\theta = 90°$; (g) bottom Closed balcony at $\theta = 0°$; (h) bottom Closed balcony at $\theta = 90°$. ————: Average IL; — — — —: lower façade average IL; –·–: upper façade average IL.

of the ceiling reflection, and higher insertion loss results on the lower half of the façade, probably because of weaker reverberation. Basically, the sound amplification appears to be the dominant mechanism at frequencies >100 Hz. There are two interesting narrow frequency bands, one at ~840 Hz and the other at ~2480 Hz, where relatively higher ILs are observed. According to the configuration used in this study (Fig. 1), there is a constructive interference between the direct sound and ground-reflected sound on the façade behind the top balcony region within the frequency range from 860 Hz to 980 Hz (M0). Therefore, at the top level, there is a high average sound pressure level on the façade without the balcony, and a relatively higher IL within the shadow zone of the balcony at frequencies near 860 Hz, regardless of the presence of the ceiling reflection [Figs. 7(b) and 8(b)]. Specular reflections take place at the balcony ceiling, but they can only reach the upper half of the façade, given the balcony geometry and source position. These reflected sounds interfere with direct sound from the source (M3), and their destructive interference so happens to fall into the frequency range from 820 Hz to 867 Hz, resulting in

high IL within the upper half of the façade. This interference does not happen in the presence of a front parapet. There are certainly interferences of direct and reflected sounds at other frequencies, but it is the right matching between these two interferences (M0 and M3) that gives rise to the high IL between 750 Hz and 860 Hz. The peak at 2480 Hz results from a similar mechanism. There can also be a case in which the frequency range of a "without balcony" destructive interference (M0) overlaps with that of a constructive interference due to the balcony ceiling reflection (M3). Such a case occurs at ~3200 Hz, resulting in an IL dip. There are other cases in which counteracting effects of these two interferences are involved. The corresponding ILs are then insignificant.

At $\theta = 45°$, the top balconies perform very similarly over the measured frequency range [Fig. 5(e)], and thus only the result of the Side-Bottom balcony is presented in Fig. 8(c). The sound interferences that take place when $\theta \neq 0°$ or 90° are much less straightforward. Discussion of these cases will be left to a future report.

The main feature of the IL of the top balconies at grazing incidence in the presence of ceiling reflection is the relatively lower IL at mid-frequencies, as shown in Fig. 5(f). The additional feature for the ILs of the balconies with side parapets is the harmonic-style large fluctuation of the one-third octave band data at higher frequencies. The IL frequency variation behind the Closed balcony is shown in Fig. 8(d). The most prominent IL dip can be observed at between 730 Hz and 800 Hz, which is mainly due to sound amplification within the balcony cavity. This amplification arises through resonance at ~743 Hz that takes place between the point of reflection on the ceiling, which is at a distance 0.7 m from the model centerline toward the nearside edge assuming specular reflection, and the far-side lower balcony corner, where strong sound amplification can be observed in Fig. 4 (M6). The length of this path is ~3 m. This resonance increases the sound intensity inside the balcony and excites a number of acoustic modes inside the cavity and near the parapet edge (where the acoustic modes for the Front-Bottom balcony should also be considered) around this frequency. This resonance leads to high sound pressure on the walls surrounding the balcony cavity, and thus to strong sound amplification. The dips at ~1460 Hz, ~2380 Hz, ~3770 Hz, and so on, are believed to be due to similar mechanisms. It should be noted that the significant ceiling reflection can only take place within the first 1 m from the near side edge at this height level, as the rest of the ceiling is shielded by the side parapet (Fig. 4).

There are also relatively significant dips at ~229 Hz and ~375 Hz. The abovementioned resonance also takes place at 228 Hz, but this frequency does not match very well with the modal characteristics of the balcony cavity, and thus the corresponding sound amplification is not very strong. A dip at ~375 Hz can also be observed in the case without ceiling reflection [Fig. 7(f)]. A resonance in the vertical direction between the ceiling and the balcony floor can occur at 381 Hz (M7), and this frequency matches with at least the eigenfrequency of a balcony cavity mode with $(m,n) = (4,2)$. Resonances and their coupling with acoustic modes appear to have significant influence on the IL spectra.

Similar wave mechanisms are expected to take place within the balconies at lower heights. In the following discussions, the more complicated Closed balcony cases are used for illustration purposes. Figures 8(e) and 8(f) present the IL spectra of the middle 'Closed' balcony at normal and grazing incidence, respectively. At $\theta = 0°$, many of the ILs dips below 1000 Hz associated with the top balcony [Fig. 8(a)] can be found in Fig. 8(e), and thus they are not discussed further. One of the major changes in the low frequency range is the addition of a ~170 Hz dip, and the dip at ~140 Hz [shown in Fig. 8(a)] is diminished. The ~170 Hz dip appears only in the results associated with balconies having a front parapet (not shown here). As more sound energy is reflected into a middle balcony by the ceiling, a vertical resonance (M7) is likely to occur between its ceiling and floor. The height of each parapet is only 0.84 m, leaving a vertical opening size of 1.35 m above the parapet. This gap creates a resonance that gives rise to high pressure on the balcony floor, and may result in a high particle velocity at a height midway between the parapet edge and the ceiling. The fundamental frequency of such resonance is 56.6 Hz, and that of its first harmonic is 169 Hz, which explains the appearance of the 168.8 Hz dip shown in Fig. 8(e).

A relatively large broadband dip can be observed between 1000 Hz to 1200 Hz. For the middle balcony, constructive interference due to ground reflection occurs within this frequency range at a height between the ceiling position and a level 1.6 m above the floor, in the absence of a balcony (M0). The presence of a reflective ceiling strengthens this effect, and thus the observed broadband IL dip. Similar phenomena take place between 2150 Hz to 2370 Hz, and between 3300 Hz to 3500 Hz. These broadband dips are also observed in the results of the other balcony forms (not shown here), further confirming that it is the ceiling that produces the sound amplification. The sharp dip of the average IL within the lower half façade at 1080 Hz is probably due to the coexcitation of many symmetric spanwise cavity modes.

Sound from the source can directly reach a location 1.6 m above the balcony floor on the façade behind the middle balcony. The interference between this direct sound and the ceiling reflection (M3) gives rise to the sharp IL peaks and dips between 1300 Hz to 2000 Hz. A strong IL peak is observed around 3100 Hz. Modal overlapping is too serious for the identification of mode contributions. There are many constructive and destructive interferences occurring at high frequencies, but most of them either do not fall into this narrow frequency range between 3000 Hz to 3200 Hz, or else they tend to smooth out their individual effects. There are many asymmetric spanwise acoustic modes with eigenfrequencies within 3100 Hz to 3200 Hz, and the number of these modes is greater than that of the symmetric modes. A similar phenomenon can be observed in Fig. 8(a) behind the top Closed balcony at ~2340 Hz.

The frequency variation of IL behind the middle Closed balcony at $\theta = 90°$, as shown in Fig. 8(f), is not much different from that of the corresponding top balcony. The major differences are that the major IL dip is found at ~700 Hz and the higher frequency IL dip at ~3550 Hz. These two dips are found in the results of all other balcony forms

included in this study. At this middle height level and orientation geometry, the ceiling cannot reflect sound directly to the lower corner of the cavity, and thus the kind of resonance described in Fig. 8(d) for the dip at ~740 Hz (M6) cannot take place within the middle balcony. However, a destructive interference due to the ground reflection occurs around the mid-height on the balcony façade at around 700 Hz, and thus the presence of the balcony disturbs such interference and increases the sound level. There is also an acoustic mode at 698 Hz (Table I) that functions in the region around the top edge of the parapets. Together with the vertical resonance that takes place at 705 Hz, an IL dip at around 700 Hz results. This pattern also applies to the IL dip at ~3500 Hz. There are sharp peaks within the frequency range from 300 Hz to 400 Hz, and their frequencies coincide with those of the cavity eigenmodes (Table I).

The broadband IL dips at around 1000 Hz and 2000 Hz are the results of constructive interference due to the ground reflection without the balcony, as shown in Fig. 8(e). The relatively regular up-and-down pattern of the IL variation between 1000 Hz to 2000 Hz is the result of the ground reflection interference (not shown here). The front parapet also receives sound directly from the sound source, and the interferences that take place at $\theta = 0°$ also occur here, but the corresponding effect is of secondary importance.

The overall IL is not significant at frequencies higher than 1500 Hz for the bottom-level balconies [Figs. 7(j), 7(k), 7(l), 8(g), 8(h)]. At the elevation level of the bottom balconies, the constructive and destructive interferences due to ground reflection occur at higher frequencies. The complicated wave interactions and modal overlapping tend to smooth each other out, making all of these effects less significant than those occurring behind the upper balconies. However, sound from the source can directly reach a location 1.2 m above the balcony floor. The frequency range of the constructive interference due to the ground reflection starts from about 1770 Hz, and extends to ~4000 Hz. This interference tends to erase all possible IL at high frequencies on the upper half of the balcony façade.

At normal incidence, the IL dips found at lower frequencies, as shown in Fig. 8(g), are found at frequencies close to those of the middle balcony [Fig. 8(e)], and thus these dips are not discussed further. The constructive and destructive interference between direct sound and the ceiling reflection within this balcony (M3) can only take place at a height greater than 1.74 m above the balcony floor, and the total balcony height is 2.19 m. The influence of such interference on IL is thus limited.

At grazing incidence, there is a broadband IL dip between 1200 Hz to 1700 Hz, as shown in Fig. 8(h). This dip is the result of destructive interference due to the ground reflection over a relatively large area, which covers the central and upper regions of the balcony façade in the absence of the balcony (M0). The broadband dip at ~4720 Hz is probably due to the same mechanism. There can be significant ground reflection interferences occurring at the lower region of the balcony façade, but the strong barrier effect and the reverberation inside the cavity should have masked their effects. As shown in Fig. 7(f), at lower frequencies the IL dips are found at frequencies close to those of the middle balcony, and these dips are thus not further discussed.

IV. CONCLUSIONS

A scale model experiment was carried out to investigate the effects of balconies and their ceilings on acoustical insertion loss in the presence of ground reflection. A three-storey balcony column was used. The effects of orientations (from normal to grazing incidence) and of elevations with respect to the noise source were also studied. Four balcony forms, namely Bottom, Side-Bottom, Front-Bottom and Closed were included. The Bottom balcony consisted of the balcony floor only and the Closed balcony had front and side parapets flanking the lower 40% of the balcony height. The Side-Bottom and Front-Bottom balconies have only side or front parapets, respectively. A long linear array consisting of 30 six-inch aperture loudspeakers was adopted as the noise source. A two-dimensional rectangular microphone array consisting of 36 equispaced 1/4 in. microphones was installed on the model façade to capture the sound pressure levels with and without the balconies.

For the balconies without ceilings, the overall A-weighted traffic noise insertion losses are affected by their configurations and their orientations relative to the sound source. As expected, the Closed and the Bottom balconies provide the highest and the lowest insertion losses, respectively. The performances of the Front-Bottom and Side-Bottom balconies show opposite variation trends as their orientations shift, but their insertion losses are roughly the same at the azimuthal angle of 45°. The effect of the azimuthal angle probably depends on the balcony floor layout, and this question is left to further investigations.

The presence of a balcony ceiling largely erases the broadband insertion losses resulting from the floor and the parapets of the balconies. For all four balcony forms tested, the variation of the insertion loss is not significant when the azimuthal angle is less than 45°, but sound amplification can be found at larger azimuthal angles. Under the current balcony configuration, the insertion losses within the second-floor balconies are generally weaker than those of other floors, because of the stronger sound reflected into the balcony region.

The insertion losses are highly dependent on frequency. For the cases without balcony ceiling reflection, the interferences between edge diffractions, diffracted waves and façade reflections appear to be the determining mechanisms for sound amplification and attenuation. The acoustic modes within balconies with a front parapet also affect the insertion losses.

The insertion losses within balconies in the presence of ceiling reflection are affected by several wave interaction mechanisms. With sound energy reflected towards the balcony floor, resonances can occur perpendicularly between the ceiling and the floor. The results also show that the interferences between sound reaching the façade directly from the sound source, sound reflected from the ground, and sound reflected from the ceiling all play important roles in shaping the frequency variations of the insertion loss. The

couplings between these mechanisms, the acoustic modes and the edge diffractions can give rise to significant sound amplifications and attenuations. At grazing incidence, the ceiling reflection hits a region near to the far-side lower corner of the top balconies with side parapets, resulting in an additional resonance and thus a strong sound amplification. This cannot occur within balconies at lower elevations. The results also relate the underlying wave behaviors and their couplings with the dimensions and elevations of the balconies.

The wave interactions within the balconies appear more complicated and much less straightforward when the balcony orientation is neither parallel with nor perpendicular to the sound source. The details of the variations in the insertion loss spectra with azimuthal angles will be presented in a separate report.

ACKNOWLEDGMENTS

The financial support of the Research Grants Council, The Hong Kong Special Administration Region Government is gratefully acknowledged (Project No. PolyU5260/12E).

[1]D. J. Oldham and E. A. Mohsan, "The acoustical performance of self-protecting buildings," J. Sound Vib. **65**, 557–581 (1979).
[2]D. N. May, "Freeway noise and high-rise balconies," J. Acoust. Soc. Am. **65**, 699–704 (1979).
[3]S. K. Tang, "Noise screening effects of balconies on a building façade," J. Acoust. Soc. Am. **118**, 213–221 (2005).
[4]C. Eveno, "A balcony in a city—Imagination in architecture," L'archit. D'Aujourd'hui **299**, 3 (1995).
[5]H. H. El-Dien and P. Woloszyn, "Prediction of the sound field into high-rise building façades due to its balcony ceiling form," Appl. Acoust. **63**, 431–440 (2004).
[6]D. C. Hothersall, K. V. Horoshenkov, and S. E. Mercy, "Numerical modeling of the sound field near a tall building with balconies near a road," J. Sound Vib. **198**, 507–515 (1996).
[7]P. J. Lee, Y. H. Kim, J. Y. Jeon, and K. D. Song, "Effects of apartment building façade and balcony design on the reduction of exterior noise," Bldg. Envrion. **42**, 3517–3528 (2007).
[8]Y. G. Tong, S. K. Tang, and M. K. L. Yeung, "Full scale model investigation on the acoustical protection of a balcony-like façade device," J. Acoust. Soc. Am. **130**, 673–676 (2011).
[9]W. Kropp and J. Bérillon, "A theoretical model to investigate the acoustic performance of building façades in low and middle frequency range," Acust. Acta Acust. **84**, 681–688 (1998).
[10]W. Kropp and J. Bérillon, "A theoretical model to consider the influence of absorbing surfaces inside the cavity of balconies," Acust. Acta Acust. **86**, 485–494 (2000).
[11]T. Ishizuka and K. Fujiwara, "Traffic noise reduction at balconies on a high-rise building façade," J. Acoust. Soc. Am. **131**, 2110–2117 (2012).
[12]H. H. El-Dien, "The influence of an inclined line source close to building façades with balconies," Noise Control Eng. J. **60**, 363–373 (2012).
[13]D. A. Naish, A. C. C. Tan, and F. N. Demirbilek, "Speech interference and transmission on residential balconies with road traffic noise," J. Acoust. Soc. Am. **133**, 210–226 (2013).
[14]S. K. Tang, "Scale model study of balcony insertion loss on a building façade with non-parallel line sources," Appl. Acoust. **71**, 947–954 (2010).
[15]C. Buratti, "Indoor noise reduction index with open window," Appl. Acoust. **63**, 431–451 (2002).
[16]M. Garai and P. Guidorzi, "European methodology for testing the airborne sound insulation characteristics of noise barriers *in situ*: Experimental verification and comparison with laboratory data," J. Acoust. Soc. Am. **108**, 1054–1067 (2000).
[17]M. E. Delany, A. J. Rennie, and K. M. Collins, "A scale model technique for investigating traffic noise propagation," J. Sound Vib. **56**, 325–340 (1978).
[18]BS EN ISO 1793-3:1998, Road traffic noise reducing devices-test methods for determining the acoustic performance—Part 3. Normalized traffic noise spectrum (International Organization for Standardization, Geneva, Switzerland, 1998).
[19]K. E. Piippo and S. K. Tang, "The characteristics of acoustic line array prototypes for scale model experiments," Appl. Acoust. **72**, 884–888 (2011).
[20]ISO 9613:1993, Acoustics—Attenuation of sound during propagation outdoors. Part 1: Calculation of absorption of sound by the atmosphere (International Organization for Standardization, Geneva, Switzerland, 1993).
[21]Z. Maekawa, "Noise reduction by screens," Appl. Acoust. **1**, 157–173 (1968).
[22]A. L'Espérance, "The insertion loss of finite length barriers on the ground," J. Acoust. Soc. Am. **86**, 179–183 (1989).
[23]Y. W. Lam and S. C. Roberts, "A simple method for accurate prediction of finite barrier insertion loss," J. Acoust. Soc. Am. **93**, 1445–1452 (1993).
[24]E. Skudrzyk, *The Foundations of Acoustics* (Wien, New York, 1971), Chap. 24, pp. 519–531.